

## <sup>10</sup>Be in quartz gravel from the Gobi Desert and evolutionary history of alluvial sedimentation in the Ejina Basin, Inner Mongolia, China

LÜ YanWu<sup>1</sup>, GU ZhaoYan<sup>1\*</sup>, ALDAHAN Ala<sup>2</sup>, ZHANG HuCai<sup>3</sup>, POSSNERT Göran<sup>4</sup> & LEI GuoLiang<sup>3</sup>

<sup>1</sup>Key Laboratory of Cenozoic Geology and Environment, Institute of Geology and Geophysics, Chinese Academy of Sciences, Beijing 100029, China;

<sup>2</sup>Department of Earth Sciences, Uppsala University, Uppsala S-75236, Sweden;

<sup>3</sup>Institute of Geography and Limnology, Chinese Academy of Sciences, Nanjing 210008, China;

<sup>4</sup>Tandem Laboratory, Uppsala University, Uppsala S-75121, Sweden

Received April 27, 2010; accepted July 13, 2010

Reconstructing the evolutionary history of the Gobi deserts developed from alluvial sediments in arid regions has great significance in unraveling changes in both tectonic activity and climate. However, such work is limited by a lack of suitable dating material preserved in the Gobi Desert, but cosmogenic <sup>10</sup>Be has great potential to date the Gobi deserts. In the present study, <sup>10</sup>Be in quartz gravel from the Gobi deserts of the Ejina Basin in Inner Mongolia of China has been measured to assess exposure ages. Results show that the Gobi Desert in the northern margin of the basin developed 420 ka ago, whereas the Gobi Desert that developed from alluvial plains in the Heihe River drainage basin came about during the last 190 ka. The latter developed gradually northward and eastward to modern terminal lakes of the river. These temporal and spatial variations in the Gobi deserts are a consequence of alluvial processes influenced by Tibetan Plateau uplift and tectonic activities within the Ejina Basin. Possible episodes of Gobi Desert development within the last 420 ka indicate that the advance/retreat of alpine glaciers during glacial/interglacial cycles might have been the dominant factor to influencing the alluvial intensity and water volume in the basin. Intense floods and large water volumes would mainly occur during the short deglacial periods.

**<sup>10</sup>Be, Gobi Desert, alluvial fan, Ejina Basin, tectonic activity, climate**

**Citation:** Lü Y W, Gu Z Y, Aldahan A, et al. <sup>10</sup>Be in quartz gravel from the Gobi Desert and evolutionary history of alluvial sedimentation in the Ejina Basin, Inner Mongolia, China. *Chinese Sci Bull*, 2010, 55: 3802–3809, doi: 10.1007/s11434-010-4103-6

The formation and evolution of an alluvial fan are closely related to variations in tectonic activity and climate. Tectonic activity often intensifies surface erosion to produce a large amount of debris. The eroded materials are transported by rivers and/or glaciers and deposited on mountain piedmont, forming vast alluvial fans. Under dry conditions, strong winds blow away the silt and sand fractions of sediments, and leave a gravel cover on the alluvial fan surface, thus forming the Gobi Desert. Abrupt floods and strong wind have been two major dynamic factors in the formation of the Gobi Desert. As a result, gravel from the Gobi Desert

has experienced both hydraulic transportation and wind erosion and would record changes in tectonic, climate, and environmental conditions. Therefore, the beginning of the development of the Gobi Desert results in the end of alluvial processes. Although many studies [1–6] have assessed alluvial fans in arid regions, the relationships of alluvial processes with tectonic activity and climate change are still unclear because of the lack of a reliable dating method. With the development of the accelerator mass spectrometry (AMS) technique in the 1980s [7–10], cosmogenic nuclide dating method has played a major role in studying landform evolution as well as climatic and environmental changes [11–18]. In this study, cosmogenic <sup>10</sup>Be measurement was

\*Corresponding author (email: zgu@mail.iggcas.ac.cn)

conducted on quartz gravel from the Gobi deserts in the Ejina Basin, Inner Mongolia, China, to understand the relationships of alluvial processes with tectonic activity and climate change.

## 1 Study area

The Ejina Basin, (40.5°–42.6°N, 99.5°–102.0°E) with an area of about  $3.4 \times 10^4$  km<sup>2</sup>, is located on the southern margin of the Mongolian Plateau northeast of the Tibetan Plateau (Figure 1). The basin is surrounded by the Dingxin Basin to the south, the Mazong Mountains to the west, the Gobi-Altai Mountains to the north, and the Badain Jaran Desert to the east. The ground has a northern aspect with a slope ranging 1‰–3‰, and altitude changes from 1130 m a.s.l. at Langxin Mountain to 890 m a.s.l. at Gaxun Nur (lake).

The large flat alluvial fan was formed in the Ejina Basin by alluvial depositions of the Heihe River (Figure 1), which originates in the Qilian Mountain at the northeastern margin of the Tibetan Plateau. It extends northward about 300 km and changes from alluvial plain to alluvial/lacustrine plain, and then to lacustrine plain [19,24,25]. The main geomorphological unit of the Ejina Basin is alluvial plain, while

lacustrine plain is distributed only in the low altitude regions of the northern basin. A series of crescent lakes including Juyanze, Gaxun Nur, and Sogo Nur are the erosion basement of the Heihe River. The terminal lake, Juyanze, dried up during the early Yuan Dynasty as a result of the river drifting westward [26]. Sogo Nur and Gaxun Nur were recharged by east and west branches of the Heihe River, respectively, before 1960 and then dried up during the 1960s because of farming in the upper and middle reaches of the Heihe River [26,27]. Additionally, a series of small alluvial fans exist on the southern piedmont of the Gobi-Altai Mountains, forming a sloping alluvial plain.

The climate of the Ejina Basin is arid. Mean annual precipitation is about 50 mm, while the mean annual potential evaporation is as high as 3700–4000 mm. The annual mean temperature of the basin is 9°C; summer is hot (28°C in July), and winter is cold (–12°C in January). Winds in the basin are strong. The basin is one of the three sandstorm centers in northwestern China [28,29], with a mean wind velocity of 4.2 m/s from April to June and a maximum of more than 20 m/s [22]. The strong winds have removed fine materials (such as sands and silts) from the surface sediment, so that the surface of the basin is almost completely covered with gravel, with depths up to tens of centimeters, this process has formed the flat, wide Gobi Desert.

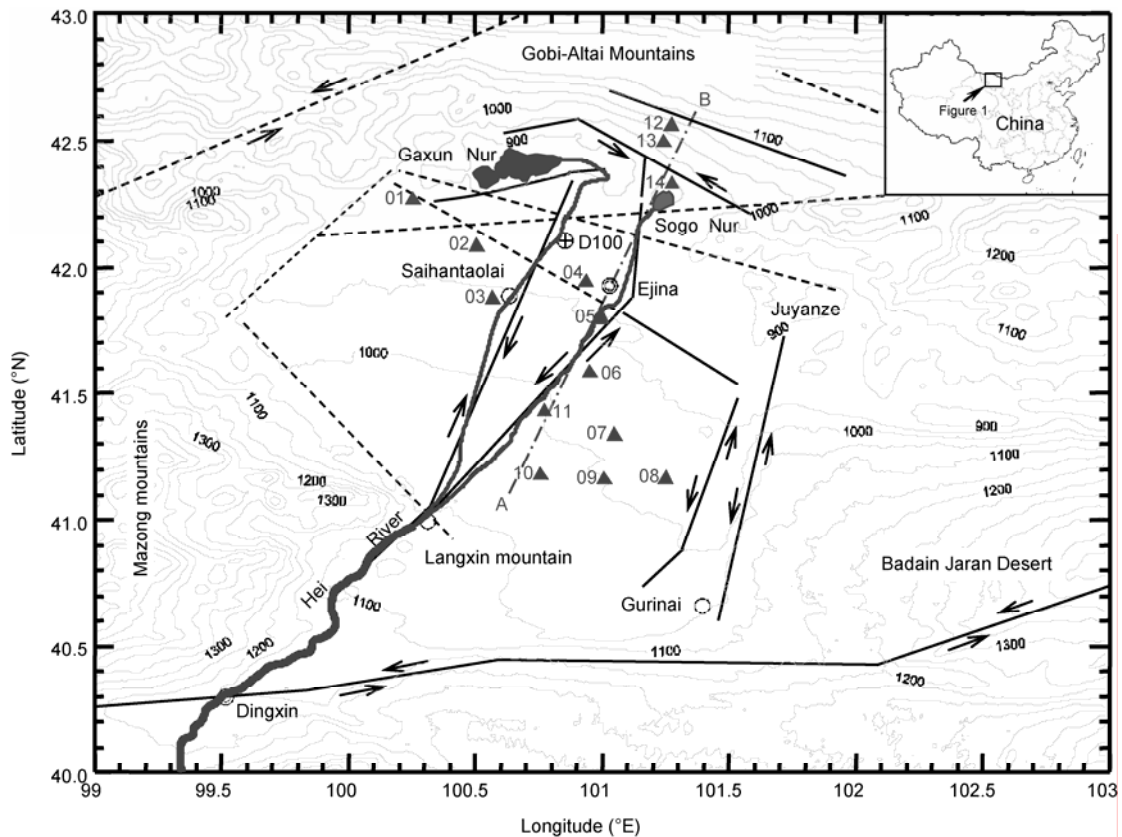


**Figure 1** Contour map of the Ejina Basin and sampling site locations. Numbers 01–14 represent samples from EJINA-01 to EJINA-14, and solid and dashed lines indicate faults and supposed faults, respectively [19–23].

## 2 Sampling and methods

A study was conducted in 2005 to investigate geology, landform, and deposition in the Ejina Basin. Fourteen quartz gravel samples were collected from the Gobi deserts along northeast and northwest transects in the basin. Two samples, EJINA-01 and EJINA-02 were taken from lacustrine platforms in the northwestern part of the basin. The platforms were 2–5 m above the plain surface [24,30], similar to the Yardang landform. Samples from EJINA-03 to EJINA-11 were collected from alluvial plains [24,30], and the EJINA-12 and EJINA-13 samples were from the sloping alluvial plain on the southern piedmont of the Gobi-Altai Mountains. The sample EJINA-14 was from gravel sediments on the modern lake beach of Sogo Nur. Except for EJINA-14, all samples were collected from areas covered by a gravel layer, 20–50 cm thick, and the underlying 2–7-m-thick sediments were composed of alluvial sands and silts with gravel. Each sample contained more than 50 pieces of quartz gravel with similar diameters and was collected from the surfaces over areas of several hectares ( $10^4$  m<sup>2</sup>). The gravel sizes of samples were different among the sites, so samples were selected in the diameter range of 2–3 cm. The sampling sites were also far from regions disturbed by human activities.

Sample preparations, including quartz purification, <sup>10</sup>Be extraction, and BeO preparation, were done in the cosmogenic nuclide laboratory at the Institute of Geology and Geophysics, Chinese Academy of Sciences. The detailed procedure is: (1) 25–40 pieces of quartz gravel were selected from each sample to reduce the influence of inherited <sup>10</sup>Be on exposure age [31–33]; (2) the gravel was crushed into 0.1–0.5 mm particles, from which equal weights were taken to mix into a sample; (3) the sample was etched

twice at 85°C in a mixed solution of 10% HF and 10% HNO<sub>3</sub> to purify the quartz and remove meteoric <sup>10</sup>Be; (4) 30 g of purified quartz with 0.3 mg of <sup>9</sup>Be carrier was digested completely in a Teflon beaker with 40% HF; (5) beryllium was separated through a cation exchange resin (Dawox 50W-X8); and (6) beryllium hydroxide was precipitated with ammonia then baked into BeO at 900°C in an oven. Three blanks were made to determine the background and to monitor the precision of the experiment processes. The <sup>10</sup>Be/<sup>9</sup>Be ratio of BeO was measured by AMS at the Tandem Laboratory of Uppsala University in Sweden. Measured ratios of <sup>10</sup>Be/<sup>9</sup>Be were normalized relative to the NIST standard-SRM4325 (<sup>10</sup>Be half-life of  $1.36 \pm 0.07$  Ma and the <sup>10</sup>Be/<sup>9</sup>Be atom ratio as  $2.79 \times 10^{-11}$  [34]). <sup>10</sup>Be concentrations of samples were calculated based on the sample weight and <sup>9</sup>Be carrier. The relative standard deviation was less than 5%.

## 3 <sup>10</sup>Be concentration and exposure ages

<sup>10</sup>Be concentrations showed high variations in amplitude in samples from the Ejina Basin (Table 1). The sample EJINA-14 from the modern lake beach of Sogo Nur had the lowest value of  $(0.53 \pm 0.03) \times 10^6$  atoms/g. The <sup>10</sup>Be concentrations for the samples of EJINA-12 and EJINA-13 samples were  $(3.63 \pm 0.10) \times 10^6$  and  $(4.14 \pm 0.09) \times 10^6$  atoms/g, respectively, and were higher than those of other samples. The <sup>10</sup>Be concentration in other samples was around  $(1.83 \pm 0.29) \times 10^6$  atoms/g.

The cosmogenic <sup>10</sup>Be in quartz was primarily produced with spallation interaction through cosmic rays bombarding oxygen atoms. The attenuation of a cosmic ray is approximately exponential when it passes through rock or is depos-

**Table 1** Measured <sup>10</sup>Be concentrations and exposure ages of the quartz gravel from the Gobi deserts in the Ejina Basin, Inner Mongolia, China

Sample	Longitude (°E)	Latitude (°N)	Elevation (m a.s.l.)	Geomorphological units	<sup>10</sup> Be concentration (10 <sup>6</sup> atoms/g)	Exposure age (ka) <sup>a)</sup>						
						M1	M2	M3	M4	M5	T <sub>app</sub>	T <sub>corr</sub>
EJINA-01	100.26	42.27	926	lacustrine low platform	1.81±0.06	203	203	203	197	194	199±8	142±9
EJINA-02	100.51	42.09	943	lacustrine high platform	2.24±0.06	252	252	252	244	240	247±9	190±9
EJINA-03	100.57	1.88	964	alluvial plain	1.37±0.05	148	148	148	144	141	145±7	89±7
EJINA-04	100.94	41.95	936	alluvial plain	1.37±0.04	152	152	152	148	145	150±6	92±7
EJINA-05	101.00	41.80	958	alluvial plain	1.77±0.07	194	194	194	188	185	190±9	134±9
EJINA-06	100.95	41.59	981	alluvial plain	1.92±0.07	210	209	208	202	199	205±9	149±9
EJINA-07	101.05	41.34	994	alluvial plain	2.09±0.08	228	226	225	219	216	221±10	166±11
EJINA-08	101.25	41.17	984	alluvial plain	1.67±0.09	180	180	179	175	172	176±10	121±11
EJINA-09	101.01	41.17	1006	alluvial plain	1.71±0.08	183	182	181	177	174	179±9	124±10
EJINA-10	100.76	41.19	1026	alluvial plain	1.97±0.07	208	206	206	200	197	202±9	149±9
EJINA-11	100.77	41.44	1004	alluvial plain	2.19±0.07	238	236	235	229	225	231±9	177±9
EJINA-12	101.27	42.57	1024	sloping Alluvial plain	3.63±0.10	397	396	296	384	380	389±14	336±15
EJINA-13	101.24	42.50	973	sloping Alluvial plain	4.14±0.09	481	484	484	470	462	475±16	420±16
EJINA-14	101.28	42.34	902	lake beach	0.53±0.03	58	59	60	58	56	58±3	0±4

a) Exposure age calculated with the online calculator of Balco et al. [35] (<http://hess.ess.washington.edu>). M1, constant production rate model [36,37]; M2–M5, time-dependent production rate mode [36–41]; T<sub>app</sub>, average exposure age and standard deviation of M2–M5; T<sub>corr</sub>, exposure age corrected for the inherited <sup>10</sup>Be of  $0.53 \pm 0.03 \times 10^6$  atoms/g.

ited on the earth's surface [42], and thus the nuclide  $^{10}\text{Be}$  in quartz is mainly produced during its exposure processes.  $^{10}\text{Be}$  concentrations ( $N$ , atoms/g) of quartz gravel in the Ejina Basin include three parts: (1) inherited  $^{10}\text{Be}$  ( $N_{\text{inh}}$ , atoms/g), which is produced during various surface processes before gravel deposition; (2) the  $^{10}\text{Be}$  produced *in situ* before exposure of gravel on the surface because of wind erosion ( $N_e$ , atoms/g); and (3) that produced *in situ* during exposure on the Gobi Desert surface ( $N_{\text{exp}}$ , atoms/g). Thus, the  $^{10}\text{Be}$  in quartz gravel of the Gobi Desert can be expressed as

$$N = N_{\text{inh}} e^{-\lambda(t_e + t_{\text{exp}})} + N_e e^{-\lambda t_{\text{exp}}} + N_{\text{exp}}, \quad (1)$$

$$N_e = \frac{P}{\lambda + \rho_1 \varepsilon_1 / \Lambda} [1 - e^{-(\lambda + \rho_1 \varepsilon_1 / \Lambda)t_e}], \quad (2)$$

$$N_{\text{exp}} = \frac{P}{\lambda + \rho_2 \varepsilon_2 / \Lambda} [1 - e^{-(\lambda + \rho_2 \varepsilon_2 / \Lambda)t_{\text{exp}}}], \quad (3)$$

where  $\lambda$  is the decay constant of  $^{10}\text{Be}$  ( $5.097 \times 10^{-6}/\text{a}$ ) [34];  $\rho_1$  and  $\rho_2$  are densities ( $\text{g}/\text{cm}^3$ ) of sediment and quartz, respectively;  $\lambda$  is the exponential mean absorption depth of cosmic rays in rocks and sediments, generally used as  $160 \text{ g}/\text{cm}^2$  [43];  $\varepsilon_1$  and  $\varepsilon_2$  are rates ( $\text{cm}/\text{a}$ ) of surface erosion before exposure of the gravel and chemical weathering of quartz on the Gobi Desert surface, respectively; and  $t_e$  and  $t_{\text{exp}}$  are the time (a) before the gravel reaches the surface and the exposure age (a), respectively.

Previous studies [44–46] have shown that the inherited  $^{10}\text{Be}$  in quartz gravel is low, e.g.  $0.15 \times 10^6$ – $0.30 \times 10^6$  atoms/g for alluvial deposits of the arid Gobi–Altai Mountains and  $0.3 \times 10^6$ – $0.7 \times 10^6$  atoms/g for alluvial deposits on the piedmont of the Qilian Mountain [47]. The  $^{10}\text{Be}$  in the sample EJINA-14 from the modern lake beach of Sogo Nur, which is within the inherited  $^{10}\text{Be}$  range of gravel from the Gobi–Altai and Qilian Mountain, would be mainly inherited for the beach formed during recent decades because of the decreasing water body area [26,27]. In theory, fine sediments should have more inherited  $^{10}\text{Be}$  than would coarse gravel; however, the  $^{10}\text{Be}$  concentration was only  $0.25 \times 10^6$  atoms/g for eolian sands from the Ejina Basin. In addition, buried gravel could be exposed to the surface for a short amount of time under strong deflation because of the loose structure of the alluvial deposits. Thus, the  $^{10}\text{Be}$  ( $N_e$ ) produced during this process should be very low. Theoretically,  $N_e$  would be less than  $1 \times 10^4$  atoms/g when the average deflation rate is more than  $1 \text{ mm}/\text{a}$  and the  $^{10}\text{Be}$  production rate is  $10 \text{ atoms}/\text{g}$ . However, this can be ignored in this study. Once exposed on the surface, gravel would remain on the surface and prevent further erosion of the underlying sediments until the next alluvial process occurred. The gravel, especially, weathering-resistant quartz gravel, would be exposed on the surface and receive cosmic ray radiation. Thus, the  $^{10}\text{Be}$  would be produced continuously. Therefore, the  $^{10}\text{Be}$  in the quartz gravel from the Gobi deserts of the

Ejina Basin are mainly produced after the formation of the Gobi Desert, and the concentration of  $^{10}\text{Be}$  is a function of the exposure time.

Exposure ages, as defined in [36,48], were calculated using the online calculator of Balco et al. [35] (<http://hess.ess.washington.edu>). Assuming the diameter of quartz gravel to be the sampling thickness, the exposure ages for different models of M1–M5 are calculated without any correction for  $N_{\text{inh}}$ ,  $N_e$ , and weathering of the gravel (Table 1). The differences among them for a given sample are less than 5% and are within the AMS measured uncertainties. The present study adopted a mean value of the exposure ages for the four time-dependent production rate models. The errors were the combinations of measurement uncertainties and accumulated standard deviations produced by the models, without considering the errors of  $^{10}\text{Be}$  half-life and production rate. Taking the  $^{10}\text{Be}$  concentration of the quartz gravel from the lake beach as the inherited  $^{10}\text{Be}$  for other samples, the corrected ages would be about 56 ka younger than those without correction. Hereinafter, exposure ages are the corrected ages.

The corrected exposure ages derived from the  $^{10}\text{Be}$  concentrations of the quartz gravel in the Ejina Basin are related with geomorphological units and altitudes (Figure 2). The ages of the gravel from the alluvial plains in the drainage basin of the Heihe River show a positive correlation with altitude ( $r = 0.65$ ), decreasing northward and eastward from 180 to 90 ka and to 123 ka, respectively (Figure 3). The ages of the gravel from the lacustrine platforms can correlate with the sequence of the platform formation, increasing from  $0 \pm 3$  ka for the lake beach, to  $142 \pm 9$  ka for the lacustrine low platform, and to  $190 \pm 9$  ka for the lacustrine high platform (Table 1). The ages of the samples of EJINA-12 and EJINA-13 from the Gobi Desert that developed from the alluvial fans in the south piedmont of the Gobi–Altai Mountains are abnormally high with a mean value of 378 ka and deviate from the distribution pattern of the exposure ages from the Gobi Desert in the drainage basin of the Heihe River.

The exposure ages of quartz gravel from the Gobi Desert would be timed for after the formation of the Gobi Desert when alluvial deposition terminated without any active river. Therefore, the exposure ages are not only represent the ages of the Gobi Desert, but could also imply the evolution of alluvial deposition. The results (Table 1) show that the Gobi Desert developed at least 420 ka ago in the northern margin of the Ejina Basin and that the Gobi Desert in the drainage basin of the Heihe River formed no more than 190 ka ago, developing toward the modern terminal lakes in the north and the low altitudes in the northeast. These ages also suggest that: (1) the arid climate occurred in the northern Ejina Basin and even in areas north of the Qilian Mountain within the last 420 ka; and (2) the alluvial deposition of sediments from the Heihe River has progressed from the south to north, while those from the Gobi–Altai Mountains

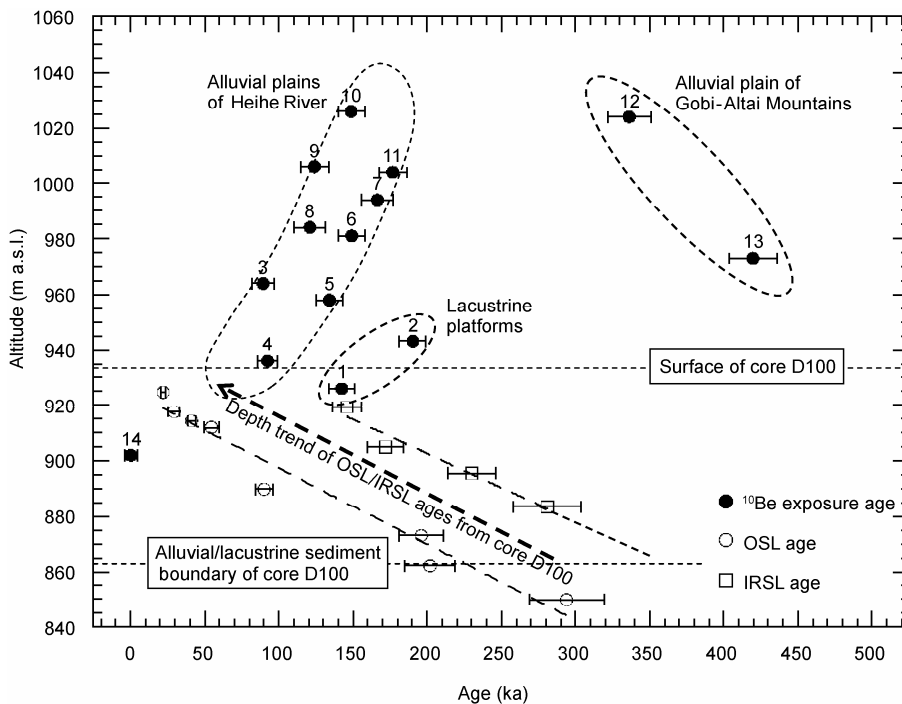


**Figure 2** Relationships of <sup>10</sup>Be exposure ages of quartz gravel from the Gobi Deserts in the Ejina Basin and OSL/IRSL ages of the core D100 [49] with altitude. Numbers 1–14 represent samples from EJINA-01 to EJINA-14.

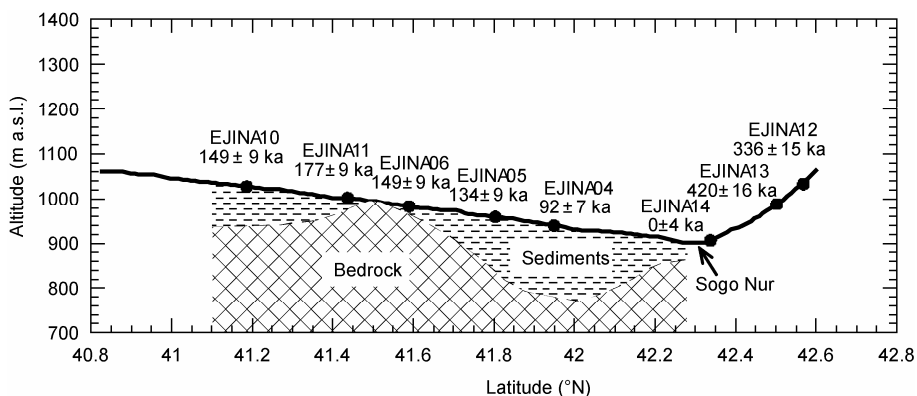


**Figure 3** Variations in altitude, sediment thickness [19], and exposure ages of the samples from the Gobi Deserts along the A-B transaction in Figure 1.

had withdrawn northwards earlier than 420 ka ago because the oldest exposure age was in the lower altitude (EJINA-13).

### 4 Discussion

The evolution of alluvial fans and their terminal lakes in drainage basins in arid regions is influenced by tectonic activities and climatic changes [50–52]. When surrounding mountains uplift and a basin subsides, the alluvial fan and lake would develop or migrate to the site of lowest altitude. The lake expands when the climate becomes humid and flooding increases; otherwise the lake shrinks. The pattern of decreasing exposure ages seen in the modern terminal lakes at low altitudes in the Ejina Basin might be a conse-

quence of the northward development of the alluvial fan associated with movement of terminal lakes as erosion basements, and/or it may be a result of tectonic uplift, rather than shrinkage of the lake because of a drying climate. Several factors lead to this conclusion.

Firstly, the northern Tibetan Plateau is a region of intense uplift [53–55]. The <sup>10</sup>Be data from the north piedmont of the Qilian Mountain indicate that the mean uplift rate was as high as 35 cm/ka during the last 170 ka [47]. The southern margin of the Ejina Basin adjoins the northern pediment of the Qilian Mountain. Thus, uplift of the plateau must drive the development of the alluvial fan in the drainage basin of the Heihe River northward.

Secondly, the original deposition centers of the Ejina Basin were not the modern terminal lakes of Juyanze, Sogo

Nur, and Gaxun Nur. Evidence from drilling cores has shown that the ancient Heihe River formed two branches in the Ejina Basin. They flowed into two ancient deposition centers including Gurinai in the southeastern basin and Saihantaolai in the central basin (Figure 1). The sediment thickness in the two deposition centers is as high as 340 m but gradually decreases with increasing distance from the deposition center [56–58]. Even bedrock can be seen at the site located at 41.49°N, 100.93°E (Figures 1 and 3). The modern terminal lakes are located far from the two ancient deposition centers, where sediments are thin and range from 40–60 m. Without considering tectonic activities, the bedrock altitudes of Gurinai and Saihantaolai are about 670 m and 620 m a.s.l., respectively, and are much lower than those of the modern terminal lakes (about 855 m a.s.l.) (Figure 3). Therefore, the modern terminal lakes are migrations of the two ancient deposition centers. Additionally, the sediment core D100 (934 m a.s.l.) located 20 km northeast of Saihantaolai (Figure 1) shows where sediments had accumulated up to a depth of about 230 m on the basin basement [49]. The core was composed of (1) laminated lacustrine silt-clay sediments at depths between 71 and 229 m, (2) interbedded layers with eolian, alluvial, and lacustrine sediments at depths from 7 to 71 m, and (3) gravel in the top 7 m. According to the OSL/IRSL ages [49], alluvial deposition at this site started about 290±50 ka ago when the terminal lake migrated northwards, and ended during the last glacial period. The fact that the age of the surface sediment at the site of core D100 is in the 934 m a.s.l. range of <sup>10</sup>Be exposure ages (Figure 2) further suggests that tectonic uplift and alluvial sediment accumulation are the major factors for the northward movement of the terminal lakes.

Finally, deposits in the Ejina Basin have been severely affected by tectonic activities. Although a basin is often thought of as a relatively stable plate, recent studies [20,21,23,59] including remote sense surveys [22,60,61] indicate that tectonic activities have influenced sedimentation in the Ejina Basin. The thin sediment belt along the northeast-southwest transect enclosing the exposed bedrock (41.49°N, 100.93°E), could be a result of basement uplifting [57,62]. The <sup>10</sup>Be exposure ages of the Gobi Desert around the bedrock outcrop are the oldest of those in the Heihe River drainage basin and decrease with increasing sediment thickness (Figure 1). This is apparently consistent with alluvial deposition occurring toward a tectonic subsidence region. Therefore, these <sup>10</sup>Be data not only supported the interpretation of tectonic activities in the Ejina Basin by remote sensing [22,60,61] but also explain the relatively low correlation between exposure ages and altitudes (Figure 2).

The lacustrine terrace or platform can result from tectonic uplift and climate changes. The exposure ages of lacustrine platforms in the northwestern basin seemingly support the assumption that lake water level was high and stable around 190±9 ka and 142±9 ka ago, respectively. Based on the modern altitude of the lacustrine high platform (943 m a.s.l.), lake areas would have reached 10<sup>4</sup> km<sup>2</sup> at that time. If the above assumption was correct, the site of core

D100 would be covered with deep water because the paleoaltitude of the sediment surface was around 875–905 m a.s.l. at 190 ka based on OSL/IRSL ages [49]. However, the fact that the sediments deposited during this interval are interbedded with layers of eolian, alluvial, and lacustrine sediments indicates a shallow water and/or dry deposition environment. The typical lacustrine sediments were deposited before 290±50 ka ago and buried more than 71 m belowground (Figure 2). In addition, the surface materials in the eastern basin at the same altitude (943 m a.s.l.) as the lacustrine platform are alluvial and eolian sediments without lacustrine sediments. The geomorphological map shows one riverine scarp and two lacustrine scarps in the north-south direction, between the west branch of the modern Heihe River and the EJINA-02 sample site [30]. It may be reasonable that the northwest lacustrine platforms were uplifted relative to the Saihantaolai deposition center and Heihe River. Landform investigations [24,30] have supported the assertion that some of the lacustrine platforms in the Juyanze region formed because of tectonic activities.

The influence of climate-controlled water recharge on the evolution of sedimentary geomorphology cannot be ignored despite tectonic activities playing a major role. The Heihe River originated from the Qilian Mountain and was supplied by ice melt. Theoretically, the advance and retreat of glaciers on the mountains would substantially influence the inflow of the Heihe River, alluvial intensity, and the areas of terminal lakes in the Ejina Basin. The <sup>10</sup>Be exposure ages from alluvial fans on the northern piedmont of the Gobi-Altai Mountains are highly correlated with the glacial terminations of MIS (Marine Isotope Stages) 2, 6, 8, and 10 [45]. In this study, the two exposure ages of 336±15 ka and 420±16 ka from the Gobi Desert in the Gobi-Altai alluvial plains also correlated with glacial terminations of MIS 10 and 12, respectively (Figure 4). The <sup>10</sup>Be exposure ages from

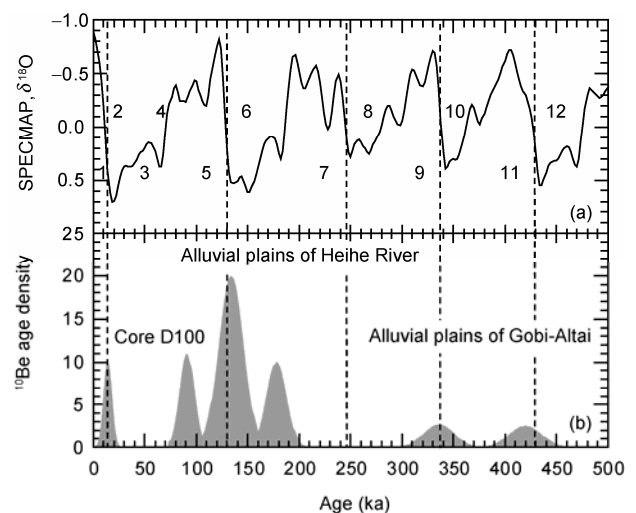


**Figure 4** SPECMAP of marine isotope records (a) and <sup>10</sup>Be exposure age distribution of Gobi Desert quartz gravel in the Ejina Basin (b). Numbers 1–12 denote marine isotope stages (MIS), and the dashed lines are the glacial/interglacial boundaries.

alluvial plains in the drainage basin of the Heihe River that were concentrated at  $134\pm 30$  ka and the top 7 m gravel layer of core D100 that was formed about 14 ka ago [49] were correlated with the glacial terminations of MIS 6 and 2, respectively (Figure 4). Although exposure age is defined as the inactive alluvial time, in the Gobi Desert it could be regarded as the age of the last alluvial process because the time for Gobi formation was short under arid and windy conditions. Thus, the distribution (Figure 4) of the  $^{10}\text{Be}$  exposure ages from the Gobi Desert implies that deglacial intervals would be the main alluvial periods and short intervals of high lake levels in the Ejina Basin. Therefore, climate during glacial/interglacial cycles may have been the main factor regulating alluvial intensity, and tectonic activity may have been an important factor in the spatial distribution of alluvial sediments.

## 5 Conclusions

The history of the development of the Gobi Desert in the Ejina Basin has been reconstructed based on the measured cosmogenic nuclide  $^{10}\text{Be}$  in quartz gravel. Results indicate that tectonic activity and climate changes have influenced alluvial processes and evolution of the alluvial fan and terminal lakes. The arid Gobi Desert landscape occurred on the alluvial plain of the Gobi-Altai Mountains on the northern margin of the Ejina Basin at least 420 ka ago, while the Gobi Desert on alluvial plains of the drainage basin of the Heihe River have developed within the last 190 ka. Northward movement of the terminal lakes with development of the alluvial fan could be influenced by Tibetan Plateau uplift and tectonic activities within the Ejina Basin. The advance and retreat of glaciers on the Qilian Mountain during glacial/interglacial cycles dominate the intensity of alluvial processes and water body dynamics. Intense floods and large water volume in the Ejina Basin might have occurred during deglacial periods.

*The authors would like to thank the Tandem Laboratory of Uppsala University in Sweden for  $^{10}\text{Be}$  measurement and financial support. Thanks also go to Dr. Yongfu Chen (IGGCAS) for his fieldwork and Daowen Wang (IGGCAS) for his help with BeO preparation. This work was supported by the Knowledge Innovation Program of the Chinese Academy of Sciences (KZCX2-YW-117) and the National Natural Science Foundation of China (40841022 and 40373046).*

- McFadden L D, Wells S G, Jercinovich M J. Influences of eolian and pedogenic processes on the origin and evolution of desert pavements. *Geology*, 1987, 15: 504–508
- Cooke R U, Warren A, Goudie A S, et al. *Desert Geomorphology*. London: UCL Press, 1993. 1–4
- Wang G Y, Dong G R, Li S, et al. An approaching discussion on Gobi plane and its facies significance (in Chinese). *J Desert Res*, 1995, 15: 124–130
- Feng Z D, Chen F H, Tang L Y, et al. East Asian monsoon climates and Gobi dynamics in marine isotope stages 4 and 3. *Catena*, 1998, 33: 29–46
- Jiang X S, Pan Z X. Gobi sediments in the Cretaceous desert of China (in Chinese). *J Mineral Petrol*, 2001, 21: 74–80
- Feng Z D. Gobi dynamics in the Northern Mongolian Plateau during the past 20000+ yr: Preliminary results. *Quat Int*, 2001, 76/77: 77–83
- Nishiizumi K, Lal D, Klein J, et al. Production of  $^{10}\text{Be}$  and  $^{26}\text{Al}$  by cosmic rays in terrestrial quartz in situ and implications for erosion rates. *Nature*, 1986, 319: 134–136
- Klein J, Giegengack R, Middleton R, et al. Revealing histories of exposure using *in situ* produced  $^{26}\text{Al}$  and  $^{10}\text{Be}$  in Libyan Desert Glass. *Radiocarbon*, 1986, 28: 547–555
- Cerling T E, Craig H. Geomorphology and in-situ cosmogenic isotopes. *Annu Rev Earth Planet Sci*, 1994, 22: 273–317
- Gosse J C, Phillips F M. Terrestrial in situ cosmogenic nuclides: Theory and application. *Quat Sci Rev*, 2001, 20: 1475–1560
- Bierman P R, Gillespie A R, Caffee M W. Cosmogenic ages for earthquake recurrence intervals and debris flow fan deposition, Owens Valley, California. *Science*, 1995, 270: 447–450
- Gu Z Y, Lal D, Liu T S, et al. Five million year  $^{10}\text{Be}$  record in Chinese loess and red-clay: Climate and weathering relationships. *Earth Planet Sci Lett*, 1996, 144: 273–287
- Siame L L, Bourlès D L, Sèbrier M, et al. Cosmogenic dating ranging from 20 to 700 ka of a series of alluvial fan surfaces affected by the El Tigre fault, Argentina. *Geology*, 1997, 25: 975–978
- Gu Z Y, Lal D, Liu T S, et al. Weathering histories of Chinese loess deposits based on uranium and thorium series nuclides and cosmogenic  $^{10}\text{Be}$ . *Geochim Cosmochim Acta*, 1997, 61: 5221–5231
- Nichols K K, Bierman P R, Hooke R L, et al. Quantifying sediment transport on desert piedmonts using  $^{10}\text{Be}$  and  $^{26}\text{Al}$ . *Geomorphology*, 2002, 45: 105–125
- Nishiizumi K, Caffee M W, Finkel R C, et al. Remnants of a fossil alluvial fan landscape of Miocene age in the Atacama Desert of northern Chile using cosmogenic nuclide exposure age dating. *Earth Planet Sci Lett*, 2005, 237: 499–507
- Vassallo R, Ritz J F, Braucher R, et al. Dating faulted alluvial fans with cosmogenic  $^{10}\text{Be}$  in the Gurvan Bogd mountain range (Gobi-Altay, Mongolia): Climatic and tectonic implications. *Terra Nova*, 2005, 17: 278–285
- Gu Z Y, Xu B, Lu Y W, et al. The geomorphological evolution of Nujiang Gorge: Preliminary results from cosmogenic dating of terrace (in Chinese). *Quat Sci*, 2006, 26: 293–294
- Zhang H C, Ming Q Z, Lei G L, et al. Dilemma of dating on lacustrine deposits in an hyperarid inland basin of NW China. *Radiocarbon*, 2006, 48: 219–226
- Hölz S, Polag D, Becken M, et al. Electromagnetic and geoelectric investigation of the Gurinai Structure, Inner Mongolia, NW China. *Tectonophysics*, 2007, 445: 26–48
- Hartmann K, Wünnemann B. Hydrological changes and Holocene climate variations in NW China, inferred from lake sediments of Juyanze palaeolake by factor analyses. *Quat Int*, 2009, 194: 28–44
- Wang X Y, Guo H D, Chang Y M, et al. On paleodrainage evolution in mid-late Epipleistocene based on radar remote sensing in northeastern Ejina Banner, Inner Mongolia. *J Geograph Sci*, 2004, 14: 235–241
- Becken M, Hölz S, Fiedler-Volmer R, et al. Electrical resistivity image of the Jingsutu Graben at the NE margin of the Ejina Basin (NW China) and implications for the basin development. *Geophys Res Lett*, 2007, 34: L09315
- Chi Z Q, Wang Y, Yao P Y, et al. Tectonic and climatic events recorded by morphologic units in Ejina Qi, Inner Mongolia (in Chinese). *Geol Rev*, 2006, 52: 370–378
- Ma J Z, Ding Z, Gates J B, et al. Chloride and the environmental isotopes as the indicators of the groundwater recharge in the Gobi Desert, northwest China. *Environ Geol*, 2008, 55: 1407–1419
- Ma Y, Cao X Q, Li Z P. Environment changes and its dynamic mechanism of Ejina region in the lower reaches of Heihe River (in Chinese). *Meteorol Environ Sci*, 2008, 31: 44–47
- Xiao S C, Xiao H L. The impact of human activity on the water environment of Heihe water basin in last century (in Chinese). *J Arid*

- Land Resour Environ, 2004, 18: 57–62
- 28 Hu J M, Cui H T, Tang Z Y. Temporal and spatial characteristics of sandstorm in China and the influences of human activities on its development trend (in Chinese). *J Nat Disast*, 1999, 8: 49–56
  - 29 Shi P J, Yan P, Gao S Y, et al. The duststorm disaster in China and its research progress (in Chinese). *J Nat Disast*, 2000, 9: 71–77
  - 30 Editorial board of The People's Republic of China Landform Atlas. The People's Republic of China Landform Atlas (in Chinese). Beijing: Science Press, 2009
  - 31 Anderson R S, Repka J L, Dick G S. Explicit treatment of inheritance in dating depositional surfaces using *in situ*  $^{10}\text{Be}$  and  $^{26}\text{Al}$ . *Geology*, 1996, 24: 47–51
  - 32 Repka J L, Anderson R S, Finkel R C. Cosmogenic dating of fluvial terraces, Fremont River, Utah. *Earth Planet Sci Lett*, 1997, 152: 59–73
  - 33 Hancock G S, Anderson R S, Chadwick O A, et al. Dating fluvial terraces with  $^{10}\text{Be}$  and  $^{26}\text{Al}$  profiles: Application to the Wind River, Wyoming. *Geomorphology*, 1999, 27: 41–60
  - 34 Nishiizumi K, Imamura M, Caffee M W, et al. Absolute calibration of  $^{10}\text{Be}$  AMS standards. *Nucl Inst Meth B*, 2007, 258: 403–413
  - 35 Balco G, Stone J O, Lifton N A, et al. A complete and easily accessible means of calculating surface exposure ages or erosion rates from  $^{10}\text{Be}$  and  $^{26}\text{Al}$  measurements. *Quat Geochronol*, 2008, 3: 174–195
  - 36 Lal D. Cosmic ray labeling of erosion surface: *in situ* nuclide production rates and erosion models. *Earth Planet Sci Lett*, 1991, 104: 424–439
  - 37 Stone J O. Air pressure and cosmogenic isotope production. *J Geophys Res*, 2000, 105: 23753–23759
  - 38 Desilets D, Zreda M. Spatial and temporal distribution of secondary cosmic-ray nucleon intensities and applications to *in situ* cosmogenic dating. *Earth Planet Sci Lett*, 2003, 206: 21–42
  - 39 Desilets D, Zreda M, Prabu T. Extended scaling factors for *in situ* cosmogenic nuclides: New measurements at low latitude. *Earth Planet Sci Lett*, 2006, 246: 265–276
  - 40 Dunai T J. Influence of secular variation of the geomagnetic field on production rates of *in situ* produced cosmogenic nuclides. *Earth Planet Sci Lett*, 2001, 193: 197–212
  - 41 Lifton N A, Bieber J W, Clem J M, et al. Addressing solar modulation and long-term uncertainties in scaling secondary cosmic rays for *in situ* cosmogenic nuclide applications. *Earth Planet Sci Lett*, 2005, 239: 140–161
  - 42 Lal D. *In situ*-produced cosmogenic isotopes in terrestrial rocks. *Ann Rev Earth Planet Sci*, 1988, 16: 355–388
  - 43 Lal D. Cosmic ray produced isotopes in terrestrial systems. *P Indian Acad Sci (Earth Planet Sci)*, 1998, 107: 241–249
  - 44 Ritz J F, Bourlès D L, Brown E T, et al. Late Pleistocene to Holocene slip rates for the Gurvan Bulag thrust fault (Gobi-Altay, Mongolia) estimated with  $^{10}\text{Be}$  dates. *J Geophys Res*, 2003, 108: ETG8-1-ETG8-16
  - 45 Vassallo R, Ritz J F, Braucher R, et al. Dating faulted alluvial fans with cosmogenic  $^{10}\text{Be}$  in the Gurvan Bogd mountain range (Gobi-Altay, Mongolia): Climatic and tectonic implications. *Terra Nova*, 2005, 17: 278–285
  - 46 Ritz J F, Vassallo R, Braucher R, et al. Using *in situ*-produced  $^{10}\text{Be}$  to quantify active tectonics in the Gurvan Bogd mountain range (Gobi-Altay, Mongolia). *Geol Soc Am Bull*, 2006, spe415-06: 87–109
  - 47 Hetzel R, Niedermann S, Tao M X, et al. Low slip rates and long-term preservation of geomorphic features in Central Asia. *Nature*, 2002, 417: 428–432
  - 48 Gu Z Y, Liu T S, Lal D. Application of the *in situ* cosmogenic nuclides  $^{10}\text{Be}$  and  $^{26}\text{Al}$  for studies of formation and evolutionary histories of the Earth surface (in Chinese). *Quat Sci*, 1997, 3: 211–221
  - 49 Wünnemann B, Altmann N, Hartmann K, et al. Interglacial and Glacial fingerprints from lake deposits in the Gobi Desert, NW China. In: Sirocko F, Clausen M, Sanchez-Goni M, eds. *The Climate of the Past Interglacials*. Amsterdam: Elsevier, 2005. 323–347
  - 50 Harvey A M. The occurrence and role of arid zone alluvial fans. In: Thomas D S, ed. *Arid Zone Geomorphology*. London: Belhaven Press, 1989. 136–158
  - 51 Ritter J B, Miller J R, Enzel Y, et al. Quaternary evolution of Cedar Creek alluvial fan, Montana. *Geomorphology*, 1993, 8: 287–304
  - 52 Harvey A M, Mather A E, Stokes M. *Alluvial Fans: Geomorphology, Sedimentology, Dynamics*. London: Geological Society, Special Publications, 2005, 251: 1–7
  - 53 Tapponnier P, Xu Z Q, Roger F, et al. Oblique stepwise rise and growth of the Tibet Plateau. *Science*, 2001, 294: 1671–1677
  - 54 Zheng W T, Yang J C, Duan F J. A study on the relation between deformation of river terraces and neotectonic activity for the Wuwei Basin (in Chinese). *Seismol Geol*, 2000, 22: 318–328
  - 55 Pan B T, Wu G J, Wang Y X, et al. Age and genesis of the Shagou River terraces in eastern Qilian Mountain. *Chinese Sci Bull*, 2001, 46: 509–513
  - 56 Gong J D, Cheng G D, Zhang X Y, et al. Environmental changes of Ejina region in the lower reaches of Heihe River (in Chinese). *Adv Earth Sci*, 2002, 17: 491–496
  - 57 Wen X, Wu Y, Su J, et al. Hydrochemical characteristics and salinity of groundwater in the Ejina Basin, Northwestern China. *Environ Geol*, 2005, 48: 665–675
  - 58 Si J H, Feng Q, Wen X H, et al. Major ion chemistry of groundwater in the extreme arid region of northwest China. *Environ Geol*, 2009, 57: 1079–1087
  - 59 Hartmann K, Wünnemann B, Zhang H C. Evidence of neotectonic impact on a large sedimentary basin between Tibetan Plateau and Gobi Altay, NW China. *Quat Sci*, 2009, 29: 687–695
  - 60 Guo H D, Liu H, Wang X Y, et al. Subsurface old drainage detection and paleoenvironment analysis using spaceborne radar images in Alxa Plateau. *Sci China Ser D Earth Sci*, 2000, 43: 439–448
  - 61 Wang X Y, Guo H D, Shao Y, et al. Analysis of shallow groundwater based on SIR-C data in north Ejina County of Inner Mongolia (in Chinese). *J Rem S*, 2002, 6: 523–526
  - 62 Zhang Y H, Wu Y Q, Su J P, et al. Mechanism of groundwater replenishment in Ejina Basin (in Chinese). *J Des Res*, 2006, 26: 96–102